Journal of Nuclear Materials 378 (2008) 238–243

Contents lists available at ScienceDirect

Journal of Nuclear Materials

journal homepage: www.elsevier.com/locate/jnucmat

Processing of uranium oxide and silicon carbide based fuel using polymer infiltration and pyrolysis

Abhishek K. Singh, Suraj C. Zunjarrao, Raman P. Singh *

Mechanics of Advanced Materials Laboratory, School of Mechanical and Aerospace Engineering, Oklahoma State University, Stillwater, OK 74078, USA

ARTICLE INFO

Article history:
Received 25 July 2007
Accepted 9 April 2008

ABSTRACT

Ceramic composite pellets consisting of uranium oxide, UO_2, contained within a silicon carbide matrix, were fabricated using a novel processing technique based on polymer infiltration and pyrolysis (PIP). In this process, particles of depleted uranium oxide, in the form of U_3O_8, were dispersed in liquid allylhydridopolycarbosilane (AHPCS), and subjected to pyrolysis up to 900 °C under a continuous flow of ultra high purity argon. The pyrolysis of AHPCS, at these temperatures, produced near-stoichiometric amorphous silicon carbide (*a*-SiC). Multiple polymer infiltration and pyrolysis (PIP) cycles were performed to minimize open porosity and densify the silicon carbide matrix. Analytical characterization was conducted to investigate chemical interaction between U_3O_8 and SiC. It was observed that U_3O_8 reacted with AHPCS during the very first pyrolysis cycle, and was converted to UO_2. As a result, final composition of the material consisted of UO_2 particles contained in an *a*-SiC matrix. The physical and mechanical properties were also quantified. It is shown that this processing scheme promotes uniform distribution of uranium fuel source along with a high ceramic yield of the parent matrix.

1. Introduction

Ceramic based fuels are preferred for gas-cooled reactors where the in-core temperature can be as high as 1200 °C during normal reactor operation and may exceed 1700 °C in case of an accident [1]. Furthermore, fuel elements should have high mechanical strength to endure various external mechanical loads, irradiation, and thermal stresses, while maintaining their integrity [2]. Given these requirements, ceramic materials are good candidates for nuclear fuels and in-core materials.

Of the various advanced ceramics, silicon carbide has superior characteristics as a structural material from the viewpoint of its thermal and mechanical properties, thermal shock resistance, chemical stability, and low radioactivation [3,4]. Therefore, there have been many efforts to develop SiC based composites in various forms for use in advanced energy systems [5,6]. Alkan et al. [5] proposed a joining technique of SiC parts so that the fissile material could be encapsulated in SiC capsules. Lee et al. [6] studied the effect of cyclic thermal shock on the mechanical and thermal properties of various ceramics being considered as candidates for nuclear fuel matrices. They observed that the silicon carbide based material exhibited superior mechanical and thermal shock performance at higher temperatures, as compared to those based on zirconia or magnesia aluminate.

The effect of high temperature irradiation on swelling and mechanical properties of high purity SiC has also been evaluated by various researchers. Raffrey et al. found that high cycle efficiency and safety considerations make SiC/SiC materials attractive for use as high performance blankets with LiPb [7]. While the irradiation stability of SiC has always been of concern, it has been established that suitable properties are expected when the composition of silicon carbide is close to stoichiometric and the microstructure is crystalline [4,8–13]. In a recent study, Hinoki et al. found excellent high temperature irradiation resistance for high purity SiC/SiC composites irradiated up to 1600 °C [4], Moreover, Newsome et al. [12] reported insignificant degradation in mechanical properties for high purity silicon carbide after irradiation. They found that the magnitude of volumetric swelling depended on the irradiation temperature and material, and was nearly independent of the irradiation fluence.

Such properties make SiC a promising candidate for use in nuclear applications. However, there are several requirements for the successful application of this material. First, the fabrication process must allow control over microstructure and material purity to ensure performance under high temperature and irradiation environments. Second, the processing technique should allow for facile incorporation of reinforcements and net shape manufacturing. Finally, a non-powder based method would be preferable for

* Corresponding author.
E-mail address: raman.singh@okstate.edu (R.P. Singh).

0022-3115/$ - see front matter © 2008 Elsevier B.V. All rights reserved.
doi:10.1016/j.jnucmat.2008.04.022

processing techniques that involve the handling of highly radiotoxic materials.

Typical manufacturing of ceramic products is based on shaping and consolidation of fine ceramic powders. Large sintering shrinkage of 15–20% limits geometrical accuracy; therefore, machining is often needed to achieve precision and intricacy. Furthermore, very high temperatures or pressures, required during sintering, hinder the incorporation of reinforcements such as silicon carbide fibers. As an alternative ceramic fabrication process, polymer infiltration and pyrolysis (PIP), offers direct control of the microstructure and composition; allows for incorporation of fibrous and particulate reinforcements; and, perhaps most importantly, offers the possibility of net shape manufacturing at temperatures as low as 500–1500 °C [14–16]. In this manner, the fabrication of ceramic components through PIP is a flexible and a potentially cost efficient approach. Finally, this process offers the unique possibility of modifying the structure and composition, and thereby the properties of ceramics, by designing the chemistry of the polymer precursor [17].

Polymer infiltration and pyrolysis has been identified as a viable alternative for fabricating SiC based materials by various researchers [14–16,18–22]. However, the use of PIP for fabricating materials targeted for nuclear applications is limited. This paper reports on a study to fabricate silicon carbide and uranium oxide based nuclear fuels using the PIP process. Recently, Sarma et al. [22] fabricated UO_2 based fuel pellets using a combination of sintering and polymer infiltration and pyrolysis. Their approach was to infiltrate pre-sintered plugs of UO_2 using precursor derived SiC. However, unacceptable thermal conductivities were observed, possibly due to limited infiltration of the polymer precursor. In this paper, we report on a fundamentally different approach. Materials were fabricated by directly incorporating uranium oxide into the preceramic polymer, and then converting the latter to SiC by pyrolysis. In this manner, the subject process does not involve pre-sintering and can be used with any uranium or non-uranium additive [23].

2. Material fabrication

For the fabrication of fuel from natural uranium, the uranium–oxygen system is a key component. Because of required fuel stability at elevated temperatures, the oxide form of uranium is desirable. Thus, after various conversion processes of uranium ore concentrate, the final product, uranium dioxide, is used as the starting material for the nuclear fuel pellet fabrication [24]. The uranium–oxygen system has been widely studied, since the initial nuclear energy era, in order to understand the interaction of urania with its surrounding materials. Amongst various $UO_{2\pm x}$ systems, U_3O_8 is considered the most stable uranium oxide at ambient temperatures [25]. However, UO_2 is the only stable oxide of uranium at higher temperatures above 1500 °C [26] till its melting point of 2800 °C [27].

In the current study, a ceramic composite consisting of an amorphous silicon carbide (*a*-SiC) matrix containing particles of depleted uranium dioxide, UO_2, was fabricated. Allylhydridopolycarbosilane (AHPCS, commercially available as SMP-10 from Starfire Systems Inc., Malta, New York, USA) was used as the polymer precursor for producing ultra high purity silicon carbide. AHPCS is an olefin-modified polymer that undergoes pyrolysis when heated under an inert atmosphere to yield near-stoichiometric SiC. Upon heating, the polymer precursor yields a dry and partially cross-linked solid at about 300 °C. Further heating results in more cross-linking accompanied by the loss of low molecular weight oligomers and hydrogen gas until *a*-SiC is obtained at about 900 °C [28].

First, a slurry was prepared by mixing 92 wt% of U_3O_8 particles (International Bio-Analytical Industries. Boca Raton, Florida, USA) and 8 wt% of the liquid polymer precursor in a planetary ball mill (PM-100, Retsch GmbH, Haan, Germany). The composition of the initial slurry was selected so that the final material would contain ~4.99 g/cm^3 solid density of elemental uranium at the end of processing. This requirement was established by criticality calculations, carried out at Brookhaven National Laboratory, and was based on fissile loading used in the GCFBR design for the pin fuel concept [29]. An intermittent, on-off cycle of 3 min each, at 300 rpm, for 6 h was used to prepare the slurry. Such a cycle was chosen to provide adequate grinding and mixing while avoiding excessive heating. As-received U_3O_8 particles were irregular in shape (5–10 μm chunks), as shown in Fig. 1(a). The ball milling process reduced the size of the U_3O_8 particles and facilitated coating by the polymer precursor.

The liquid slurry, obtained after ball milling, was pyrolyzed in a covered alumina crucible in a box furnace. This furnace was fitted with a retort that allowed for a continuous flow of an inert gas such as nitrogen or argon. In this case, the pyrolysis was carried out under ultra high purity (UHP) argon. The slurry was heated to 900 °C at a rate of 60 °C/h, and was held at the peak temperature for 90 min to ensure thermal equilibrium. The pyrolysis of this slurry resulted in a solid that contained uranium oxide particles dispersed in an *a*-SiC matrix. However, due to the amount of polymer precursor used for this initial cycle, this solid acquired the shape of the crucible and contained large voids that were generated by the release of hydrogen gas.

In order to make cylindrical samples from this material, which could be tested for mechanical properties, the solid obtained after the above pyrolysis was crushed into powder by ball milling for 12 min at 300 rpm. The powder thus obtained was then mixed with a small amount of polymer precursor (~3% by weight of the milled powder) and compacted into short cylinders, $\phi 25.4 \times 15$ mm, using a hydraulic press. A nominal compaction pressure of

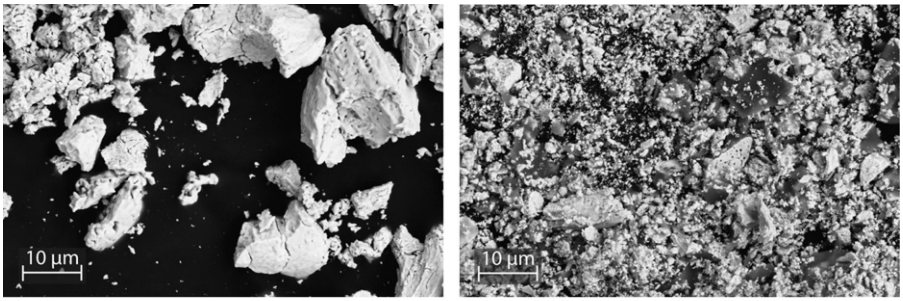

(a) As-received U_3O_8 (b) After first pyrolysis of slurry containing U_3O_8 and AHPCS

Fig. 1. Uranium particles after initial processing.

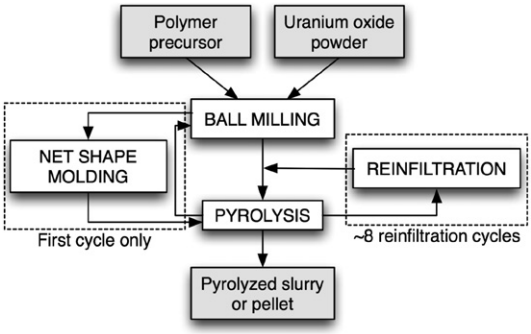

Fig. 2. Flow diagram of fuel preparation using polymer infiltration and pyrolysis.

about 26 MPa was sufficient for producing green-body plugs that could be handled for further processing. These pre-compacted plugs, in the form of short cylinders, were pyrolyzed up to 900 °C at a rate of 60 °C/h under argon.

As is customary in PIP processing, the samples were subjected to multiple polymer reinfiltration cycles. The reinfiltration of the cylindrical pellets was carried out under vacuum, with repeated 1 hour cycles for 3 h with intermediate 1 min purges. In addition, pressurized argon was used during each purge. This enhanced reinfiltration while minimizing contamination [30]. Fig. 2 shows the schematic of the PIP process used in the current study.

In the case of uranium-bearing samples, two types of composites were fabricated using different reinfiltration schemes. The first type of material, designated as *a*-SiC–U_3O_8–A, was prepared by using a mixture of polymer precursor and uranium powder (obtained after first pyrolysis and specifically ball milled for 9 h to reduce its particle size) as the reinfiltrating liquid. The second type of material, designated as (*a*-SiC–U_3O_8-B, was infiltrated using neat polymer precursor. In the first case, the use of uranium oxide particles in the infiltrating media to promote uranium loading, was stopped after the 5th reinfiltration cycle. Beyond five reinfiltrations, the pore size becomes small and the presence of uranium oxide particles in the liquid polymer precursor could impede material densification. Subsequent reinfiltrations were continued using neat polymer precursor. In the second case, all reinfiltrations were done using neat polymer precursor.

The cylindrical specimens were sliced after the 3rd reinfiltration cycle to obtain discs of 1 mm thickness using a precision sectioning saw (Isomet 1000, Buehier, Lake Bluff, Illinois, USA). Prior work with polymer derived ceramic composites, using this polymer system, has showed that ~6–8 reinfiltration cycles are sufficient to obtain the maximum achievable density [20]. Therefore reinfiltration of the discs was continued for a total of eight cycles.

To avoid oxidation of the components at any stage, all the handling and processing was carried out in an argon atmosphere. Also, control samples that contained only *a*-SiC were fabricated using the same procedure, but without the addition of any uranium oxide.

3. Physical characterization

The density and porosity of the fabricated materials was determined after the 8th reinfiltration using the buoyancy method. First the specimen was dried at 120 °C for 12 h, until it reached a constant mass, and then cooled to room temperature in a desiccator. The dry mass of the sample, m_1, was recorded. Subsequently, the dried sample was saturated using ultra-high purity water to fill all the open pores. A few drops of Photo-Flo® (Kodak Corporation, Rochester, New York, USA) were added to reduce the surface tension of water and aid in saturation. A 4 h evacuation cycle was employed with intermittent purges at every 30 min to release trapped air. The apparent mass of the saturated sample, m_2, was then determined using a density determination kit. The temperature of the saturation liquid was also recorded to correct for variations in the density of water, ρ_{fl}, as a function of temperature. Finally, the mass of the saturated sample, m_3, was determined by weighing in air. Any liquid that remained on the surface of the sample was removed with a damp sponge and the operation was performed quickly, to avoid loss of mass due to evaporation. Subsequently, the bulk density, ρ_b, was calculated as

$$\rho_b = \frac{m_1}{m_3 - m_2}\rho_{fl}, \tag{1}$$

and the open porosity, π_a, in vol.% was calculated as

$$\pi_a = \frac{m_3 - m_1}{m_3 - m_2} \times 100. \tag{2}$$

Table 1
Density and porosity of the samples after 8th reinfiltration

Material	Bulk density ρ_b (g/cm^3)	Open porosity π_a (%)
(*a*-SiC)	2.21 ± 0.01	3.39 ± 1.14
(*a*-SiC)–U_3O_8–A	4.58 ± 0.06	2.77 ± 1.14
(*a*-SiC)–U_3O_8–B	4.70 ± 0.06	1.94 ± 0.56

Bulk densities and open porosities of the samples after the 8th reinfiltration are listed in Table 1. PIP processing generated closed pores in the consolidated pellets and therefore the bulk densities of the composites obtained were lower than their true densities. The true densities of polymer derived SiC have been found to vary from 2.7 g/cm^3 at 900 °C to 3.2 g/cm^3 at 1650 °C [31]. The bulk density and porosity values for both *a*-SiC–U_3O_8–A and *a*-SiC–U_3O_8–B were found to be close. It is possible that the modified reinfiltration process, *as* for *a*-SiO–U_3O_8–A, impeded the densification leading to lower bulk density and higher open porosity, as indicated in Table 1. Given the scatter in data, however, it is not possible to make this claim unambiguously.

During fuel fabrication using sintering, the fuel pellets are produced to ~90% of the theoretical density. The deliberate introduction of residual porosity is desired in fresh fuel to accommodate fission product swelling and redistribution [32], Similarly, it is hypothesized that the presence of pores, in the current fabrication process, may decrease the effect of irradiation swelling of SiC.

Fig. 3 shows the scanning electron microscopic images of *a*-SiC–U_3O_8–A and a-SiC–U_3O_8-B, after three and eight reinfiltrations. It can be observed that the distribution of U_3O_8 (actually UO_2) was highly uniform and pores were not visible even after the third reinfiltration at this scale.

4. Mechanical testing

Mechanical characterization of the samples was carried out using biaxial flexural strength tests. Such test methods, including ring-on-ring and ball-on-3-ball, have been commonly used to characterize the flexure strength of brittle ceramic materials [33,34]. These biaxial tests are preferred over uniaxial testing (in tension or in bending) due to various reasons, which include the examination of a large surface area that is free from edge finishing defects, ease of test piece preparation, and the applicability of this method to thin sheets.

Furthermore, the biaxial stress distribution is more discriminate of material defects than a uniaxial distribution. It is hypothesized that in the biaxial flexure test method the maximum tensile stress occurs within the central loading area, and spurious edge failures are eliminated.

4.1. Biaxial flexure tests

Ring-on-ring (RoR) biaxial tests were carried out in the current investigation. The RoR is an axisymmetric test, where the disc is

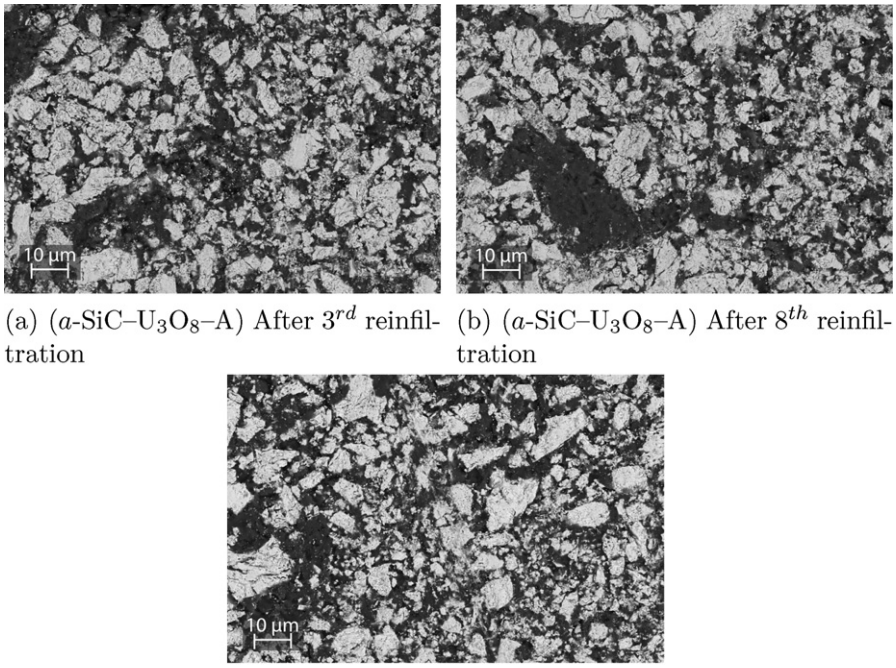

(a) (a-SiC–U_3O_8–A) After 3^{rd} reinfiltration

(b) (a-SiC–U_3O_8–A) After 8^{th} reinfiltration

(c) (a-SiC–U_3O_8–B) After 8^{th} reinfiltration

Fig. 3. Uranium ceramic composite after 3rd and 8th reinfiltrations. The bright portion of the micrograph represents UO_2 and the dark regions represent SiC matrix phase.

supported by a ring and loaded from the opposite side by another smaller concentric ring, as shown in Fig. 4. The ring-on-ring configuration is preferred over the other equibiaxial tests since it subjects a greater portion of the specimen to an equibiaxial stress state and distributes the applied contact load over a larger area. This reduces the applied stress concentration at the contact locations between the fixture and specimen and lowers the likelihood of fixture-induced specimen failure leading to invalid test data. On the other hand, there is an approximate 20% increase in the stress under the loading ring [34].

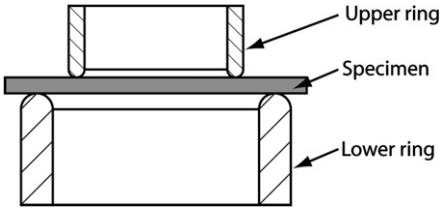

Fig. 4. RoR, flexure fixture schematic.

Care is needed to select the diameters of the loading and support rings, relative to the specimen thickness, in order to promote a valid failure event. Also, clean loading conditions and plane-parallel disk shaped specimens are required for the RoR configuration. Lack of these conditions may result in a 3-point contact between ring and specimen. The concentric rings in the current setup were made up of stainless steel and had bullnose edges with a radius of 0.3125 mm towards the loading side. This configuration employed a support ring diameter of 19.05 mm and the loading ring diameter of 6.35 mm. Fig. 5 illustrates valid tests in which the failure initiates from the central region of the discs [35].

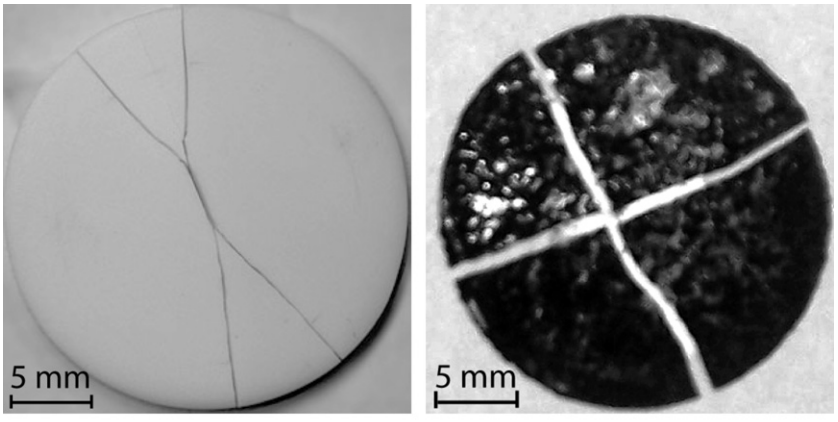

(a) Alumina disc

(b) (a-SiC)–U_3O_8–A disc

Fig. 5. Typical RoR failure.

The specimens were loaded in the RoR fixture using a table-top test frame (Instron® 5567, Instron Corporation, Norwood, Massachusetts, USA) as shown in Fig. 6. Displacement controlled loading at a rate of 0.5 mm/min was used and the peak load at failure was recorded. The flexure strength was then determined as per Eq. (3) [33],

$$\sigma_{RoR} = \frac{3P}{2\pi t^2}\left[\frac{(1-\nu)(a^2-r^2)}{2R^2} + (1+\nu)\ln\frac{a}{r}\right] \quad (3)$$

where P is the peak load at failure, ν is the Poisson ratio of the specimen and was assumed to be 0.20 for SiC, a is the radius of the support ring, r is the radius of the load ring, and R and t are the radius and thickness of the disc specimen, respectively. The validity of ring-on-ring results was examined by testing commercially obtained alumina discs (AD-90, CoorsTek, Golden, Colorado, USA). Fig. 7 shows the typical loading curve obtained for the RoR biaxial tests done on prepared discs. The flexural strength results are shown in Table 2.

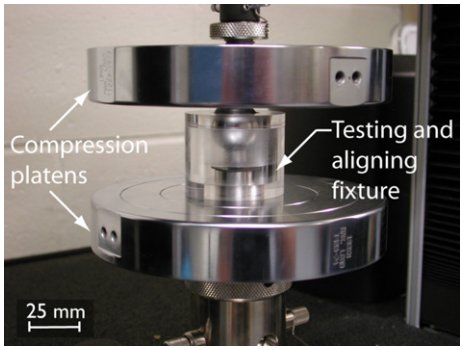

Fig. 6. Photograph of RoR fixture.

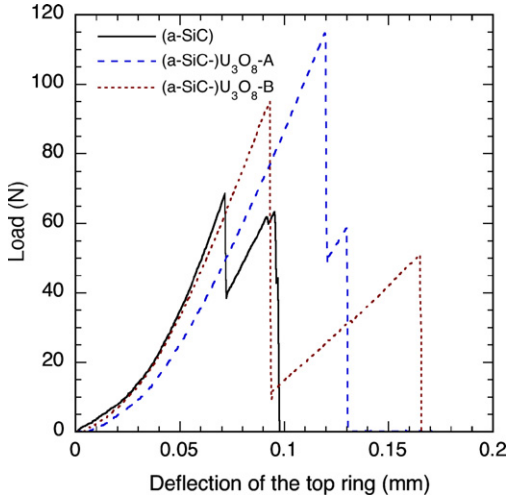

Fig. 7. Typical load–deflection curve of ceramic composites test under RoR.

Table 2
Biaxial data on composite ceramics and alumina

Sample	Filler (% Weight)	Flexure strength (MPa)
(a-SiC)	–	41.7 ± 2.1
(a-SiC)–U_3O_8–A	92	53.7 ± 3.3
(a-SiC)–U_3O_8–B	92	49.1 ± 4.5
Alumina	–	221.9 ± 17.2

Uniaxial flexure test and RoR tests were compared by Wereszczak et al. [35], on 99.5% pure alumina, samples purchased from CoorsTek. They reported that the RoR values were ~20% less than their uniaxial flexural strength. The biaxial strength obtained for alumina (AD–90, 90% purity) in our test was ~35% lower than the uniaxial strength reported by CoorsTek. However, a valid failure pattern was obtained, as suggested by Wereszczak et al. [35], for both alumina and uranium–ceramic samples, as shown in Fig. 5. The validity of these tests was identified by looking at the fracture, which originated from inside the loading ring instead of initiating beneath the ring.

Given the fact that porosity may be a desirable feature, the achievable strength will be lower than those for near theoretically-dense sintered ceramics. Surprisingly, there is a lack of published data on mechanical strength requirement for fuel pellets aimed towards GFR applications. Brittle fracture stress of approximately 1400 MPa, was reported for UO_2 based sintered fuel pellets [32]. However, this may not represent the actual physical requirement for next generation fuel pellets. To understand creep behavior, compressive stress magnitude of 41.4 MPa is typically used in literature for temperatures below 1350 °C [36]. Furthermore, the strength requirement should be studied as a function of irradiation damage, temperature and exposure time. Nonetheless, here we report the biaxial failure strength, determined at room temperature, as a means of comparing the effects of inclusions in the PIP densified SiC matrix.

5. Analytical characterization

The ceramic composite after the first pyrolysis came out as a brown cinnamon colored solid. Fig. 8 shows the as-received U_3O_8 and the pyrolyzed powder obtained after the first heating cycle. This change in color indicated a chemical conversion. Therefore, in order to investigate the microstructure and formation of new chemical species, due to *in situ* reactions, the fabricated materials were studied using powder X-ray diffraction (XRD), These measurements were performed on a Phillips PW1729/APD3520 diffractometer with CuKα radiation (λ = 0.154 nm) operating at 40 kV and 30 mA. Peaks in the XRD patterns were identified using the JCPDS-ICDD database.

Fig. 9 shows the diffraction patterns obtained for as-received U_3O_8 powder and ball milled slurry powder after one cycle of pyrolysis. The diffraction peaks in the pyrolyzed slurry pattern were mostly dominated by the presence of UO_2 providing evidence of the conversion of U_3O_8 to UO_2 during the first pyrolysis cycle. There can be various reasons for this conversion and this reduction has been widely studied [37–39]. Since the pyrolysis was carried out in an inert environment, it is highly likely that the reduction took place due to the presence of hydrogen gas that evolves during the pyrolysis of the precursor. In the presence of hydrogen this reduction can take place in the temperature range of 400–600 °C [38,39]. However, this process is highly affected by the powder properties such as BET surface area and size. A more detailed

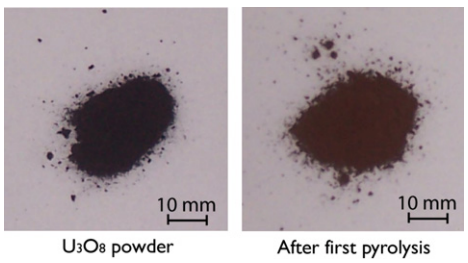

Fig. 8. Color change of parent uranium powder after first pyrolysis.

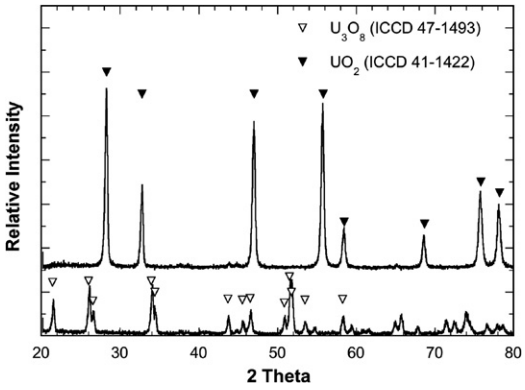

Fig. 9. X-ray diffraction pattern for as-received U_3O_8 and after first temperature cycle to 900 °C.

understanding of these redox reactions is needed. Nonetheless, the conversion of U_3O_8 to UO_2 is favorable given the stability of the latter at higher temperatures.

6. Conclusions

Composite ceramic samples containing uranium oxide powder and *a*-SiC were manufactured using the PIP technique. The starting material, U_3O_8, was converted to UO_2, as indicated by a color change and confirmed using X-ray diffraction. This conversion is advantageous as U_3O_8 is readily available and UO_2 shows better stability at higher temperatures.

Bulk densities of the composites, fabricated with our methodology, were 4.52–4.76 g/cm^3. The open porosity values were very low and highlight the efficiency of the pressure-assisted vacuum purge method. Even better densification could be obtained using pressure assisted curing of the initially compacted cylinder, as reported by Shah et al. [40] for pressure cast SiCN samples. Fairly uniform distribution of uranium particles in the specimens was observed by scanning electron microscopy.

Equibiaxial flexure strengths for samples with uranium oxide as the filler materials were higher than that for composites containing only *a*-SiC. Furthermore, it was observed that reinfiltration of the discs using a mixture of filler particles and polymer precursor led to composites with a higher load carrying capacity than those infiltrated with neat polymer precursor. This indicates the filler, with a-SiC matrix can provide strengthening mechanisms.

This composite fabrication technique holds promise for nuclear fuel preparation. However, since the pyrolysis temperature used in this study was limited to 900 °C, crystallization of SiC was not achieved. It is generally agreed that *a*-SiC, undergoes swelling under neutron irradiation, which may not be insignificant even at lower temperatures, making it unsuitable for nuclear applications. In a parallel study by Zunjarrao et al. [28], it was observed that pyrolysis to 1150–1650 °C produces β-crystalline silicon carbide from AHPCS, which would be more suitable for nuclear applications [11,12,41]. Finally it should be noted that allylhydridopolycarbosilane, the precursor used in this study, is known for its ultra high purity and ability to form near-stoichiometric SiC, which are favorable attributes for nuclear applications of SiC. In that manner, the composite prepared in this investigation could be subjected to further thermal treatment to reduce the effects of neutron irradiation.

Acknowledgements

The authors wish to thank DOE for financial support on this project (Award No. DE-FC07-05ID14673). Thanks are also due to Dr Hans Ludewig and Dr Mike Todosow, at Brookhaven National Laboratory, NY, USA, for criticality calculations. The authors gratefully acknowledge the scientific discussions with Dr John D. Metzger (Bettis Atomic Power Laboratory).

References

[1] C. Gueneau, S. Chatain, S. Gosse, C. Rado, O. Rapaud, J. Lechelle, J.C. Dumas, C. Chatillon, J. Nucl. Mater. 344 (1–3) (2005) 191.
[2] W. Corwin, L. Snead, S. Zinkle, R. Nanstad, A. Rowcliffe, L. Mansur, R. Swinderman, W. Ren, D. Wilson, T. McGreevy, P. Rittenhouse, J. Klett, T. Allen, J. Gan, K. Weaver, The gas fast reactor (GFR) survey of materials exprience and R&D needs to assess viability, Generation IV: Nuclear Energy Systems ORNL/TM-2004/99.
[3] R.H. Jones, C.H. Henager Jr., J. Euro. Ceram. Soc. 25 (10 SPEC ISS) (2005) 1717.
[4] T. Hinoki, A. Kohyama, Ann. Chim. Sci. Mater. 30 (6) (2005) 659.
[5] Z. Alkan, K. Kugeler, R. Kaulbarsch, C. Manter, Prog. Nucl. Energy 38 (3–4) (2001) 411.
[6] Y.W. Lee, S. Lee, H. Kim, C. Joung, C. Degueldre, J. Nucl. Mater. 319 (2003) 15.
[7] A.R. Raffray, L. El-Guebaiy, D.K. Sze, M. Billone, I. Sviatoslavsky, E. Mogahed, F. Najmabadi, M.S. Tillack, X. Wang, Proc. Sympos. Fusion Eng. (1999) 73.
[8] L.L. Snead, M. Osborne, K.L. More, J. Mater. Res. 10 (3) (1995) 736.
[9] D.J. Senor, G.E. Youngblood, J.L. Brimhall, D.J. Trimble, G. Newsome, J. Woods, Fusion Technol. 30 (3) (1996) 956.
[10] G.W. Hollenberg, C.H. Henager, G.E. Youngblood, D.J. Trimble, S.A. Simonson, G.A. Newsome, E. Lewis, J. Nucl. Mater. 219 (1995) 70.
[11] L.L. Snead, Y. Katoh, A. Kohyama, J. Bailey, N. Vaughn, R. Lowden, J. Nucl. Mater. 283 (2000) 551.
[12] G. Newsome, L. Snead, T. Hinoki, Y. Katoh, D. Peters, J. Nucl. Mater. 371 (1–3) (2007) 76.
[13] Y. Katoh, L.L. Snead, C.H. Henager, A. Hasegawa, A. Kohyama, B. Riccardi, H. Hegeman, J. Nucl. Mater. 367 (2007) 659.
[14] G. Peter, Adv. Eng. Mater. 101 (45) (1997) 9195.
[15] L.V. Interrante, J.M. Jacobs, W. Sherwood, C.W. Whitmarsh, Key Eng. Mater. 127–131 (Pt 1) (1997) 271.
[16] L.V. Interrante, C.W. Whitmarsh, W. Sherwood, H.J. Wu, R. Lewis, G. Maciel, Mater. Res. Soc. (1994) 593.
[17] L. Bharadwaj, Y. Fan, L. Zhang, D. Jiang, L. An, J. Am. Ceram. Soc. 87 (3) (2004) 483.
[18] A.C. Lewinsohn, H.R. Jones, P. Colombo, B. Riccardi, J. Nucl. Mater. 307–311 (2 SUPPL) (2002) 1232.
[19] M. Kotani, T. Inoue, A. Kohyama, Y. Katoh, K. Okamura, Mater. Sci. Eng. A 357 (1–2) (2003) 376.
[20] E. Ozcivici, R.P. Singh, J. Am. Ceram. Soc. 88 (12) (2005) 3338.
[21] A.K. Singh, S, C. Zunjarrao, R.P. Singh, Silicon carbide and uranium oxide based composite fuel preparation using polymer infiltration and pyrolysis, ICONE-14, ASME, Miami, Florida, USA, 2006.
[22] K.H. Sarma, J. Fourcade, S. Lee, A. Solomon, J. Nucl. Mater. 352 (1–3) (2006) 324.
[23] A.K. Singh, R.P. Singh, Fabrication of NbC, ZrC and UC based silicon carbide matrix composites for nuclear applications using polymer infiltration and pyrolysis, Material Science and Technology 2007 Conference and Exhibition, Detroit, MI, USA, 2007.
[24] S.E. Ion, R.H. Watson, E.P. Loch, Nucl. Energy 28 (1) (1989) 21.
[25] D. Labroche, O. Dugne, C. Chatillon, J. Nucl. Mater. 312 (1) (2003) 21.
[26] R. Stoops, J. Hamme, J. Am. Ceram. Soc. 47 (2) (1964) 59.
[27] E.H.P. Cordfunke, The Chemistry of Uranium, Elsevier Publishing Company, Amsterdam, Netherlands, 1969.
[28] S.C. Zunjarrao, A.K. Singh, R.P. Singh, Structure-property relationships in polymer derived amorphous/nano-crystalline silicon carbide for nuclear applications, ICONE-14, ASME, Miami, Florida, USA, 2006.
[29] B. Pellaud, The physics design of the gas cooled fast breeder reactor demonstration plant, vol. GA-10509, Gulf General Atomic Co., San Diego, CA, 1971.
[30] A.A. Solomon, P. Julien, L. Sang-Gyu, K. Sarma, R. Shripad, L. Ryan, P.L. Holinan, J. Kevin McCoy, Am. Nucl. Soc. (2004) 146.
[31] S.C. Zunjarrao, A.K. Singh, R.P. Singh, Modulus and hardness of nanocrystalline silicon carbide as functions of grain size, in: 31st International Cocoa Beach Conference and Exposition, Daytona Beach, Florida, USA, 2007.
[32] D. Orlander, Fundamental Aspects of Nuclear Reactor Fuel Elements, US Department of Energy, 1976.
[33] J.E.O. Ovri, Mater. Chem. Phys. 66 (1) (2000) 1.
[34] G. de With, H.H.M. Wagemans, J. Am. Ceram. Soc. 72 (8) (1989) 1538.
[35] A.A. Wereszczak, J.J. Swab, R.H. Kraft, Effects of machining on the uniaxial and equibiaxial flexure strength of CAP3 AD-995 Al_2O_3, ARL Technical Report, 2005.
[36] M.K. Meyer, Properties of (U, Pu)C and (U, Pu)N for use as gas-cooled fast reactor fuels, ANL-West, 2003.
[37] P. Kovacheva, D. Todorovsky, D. Radev, V. Mavrudiev, R. Petrov, D. Kovacheva, K. Petrov, J. Radioanal. Nucl. Chem. 262 (3) (2004) 573.
[38] M. Pijolat, C. Brun, F. Valdivieso, M. Soustelle, Solid State Ionics 101 (1997) 931.
[39] J.H. Yang, Y.W. Rhee, K.W. Kang, K.S. Kim, K.W. Song, S.J. Lee, J. Nucl. Mater. 360 (2) (2007) 208.
[40] S.R. Shah, R. Raj, Acta Mater. 50 (16) (2002) 4093.
[41] R.H. Jones, L. Giancarli, A. Hasegawa, Y. Katoh, A. Kohyama, B. Riccardi, L.L. Snead, W.J. Weber, J. Nucl. Mater. 307 (2002) 1057.